CASE RECORDS of the MASSACHUSETTS GENERAL HOSPITAL

Case 30-2024: A 45-Year-Old Woman with Kidney Lesions and Lytic Bone Disease

Luke Y.C. Chen, M.D., M.M.Ed., Ambrose J. Huang, M.D.,
John H. Stone, M.D., M.P.H., and Judith A. Ferry, M.D.

From the Department of Medicine, University of British Columbia, Vancouver, and Dalhousie University, Halifax, NS — both in Canada (L.Y.C.C.); and the Departments of Radiology (A.J.H.), Medicine (J.H.S.), and Pathology (J.A.F.), Massachusetts General Hospital, and the Departments of Radiology (A.J.H.), Medicine (J.H.S.), and Pathology (J.A.F.), Harvard Medical School — both in Boston.

N Engl J Med 2024;391:1140-51.
DOI: 10.1056/NEJMcpc2402486

CME

PRESENTATION OF CASE

Dr. John H. Stone: A 45-year-old woman was referred to the rheumatology clinic of this hospital because of retroperitoneal fibrosis and the possibility of IgG4-related disease.

Seven years before the current presentation, the patient had undergone a bone marrow biopsy at another hospital because of mild persistent polycythemia and leukocytosis. Examination of the biopsy specimen reportedly showed normocellular marrow with maturing trilineage hematopoiesis. No evidence of a myeloproliferative neoplasm or a V617F mutation in the gene encoding Janus kinase 2 (*JAK2*) was detected.

Five years later (2 years before the current presentation), the patient was evaluated by her primary care physician because of polycythemia and flank pain on the left side. A faint IgG kappa monoclonal band was reportedly seen on immunoelectrophoresis. The blood levels of IgG, IgA, IgM, erythropoietin, and lactate dehydrogenase were reportedly normal.

Dr. Ambrose J. Huang: Ultrasonography performed at the first hospital reportedly revealed a complicated cyst, measuring 24 mm in diameter, in the upper pole of the left kidney with mural thickening and internal echoes. The patient also had an 18-mm parapelvic cyst in the middle portion of the left kidney, a 4-mm nonobstructive calculus in the left kidney, and mild parenchymal scarring in the right kidney. Seven weeks later, magnetic resonance imaging (MRI) of the abdomen and pelvis, performed after the administration of gadolinium, allowed for further characterization of the lesions. The lesion in the upper pole of the left kidney reportedly had homogeneous enhancement and was suggestive of renal-cell carcinoma.

Approximately 17 months before the current presentation, the patient was evaluated at the urology clinic of a second hospital. Computed tomography (CT) of the abdomen and pelvis, performed after the administration of contrast material, reportedly showed the enhancing 24-mm mass in the upper pole of the left kidney that was suggestive of renal-cell carcinoma. There was no evidence of metastatic disease.

The 18-mm mass in the middle of the left kidney appeared as poorly circumscribed and hypoattenuating.

Dr. Stone: Laparoscopic partial nephrectomy was performed to remove the mass in the upper pole of the left kidney. Histopathological examination of the tissue specimen revealed mild focal global glomerulosclerosis, mild interstitial fibrosis, and mild arteriosclerosis. No tumor was seen.

Dr. Huang: Four months later, follow-up MRI of the abdomen and pelvis performed at the first hospital showed no recurrence of a mass in the surgical bed. Three months thereafter, ultrasonography performed at the first hospital reportedly revealed a new 19-mm hypoechoic lesion in the lower pole of the right kidney and showed a stable 18-mm mass in the middle of the left kidney. Gadolinium-enhanced MRI performed 1 month later showed that the 19-mm lesion in the lower pole of the right kidney was exophytic and enhancing (Fig. 1A). The appearance of this lesion on imaging was reportedly similar to the appearance of the 24-mm lesion that had been resected from the left kidney.

Dr. Stone: Approximately 7 months before the current presentation, the patient had a consultation with a urologist at a third hospital. A percutaneous CT-guided biopsy targeting the exophytic lesion in the lower pole of the right kidney was performed (Fig. 1B). On histopathological examination, there was no renal parenchyma; it was assumed that only retroperitoneal tissue near the kidney had been obtained. The biopsy specimen showed atypical fibrous tissue with a storiform pattern of fibrosis and lymphoplasmacytic inflammation. Polytypic kappa and lambda staining within plasma cells was noted. There were more than 10 IgG4+ plasma cells per high-power field, but these cells made up less than 40% of the overall IgG+ cells. Flow cytometry was performed on the tissue specimen obtained during the attempted renal biopsy and showed no monotypic B-cell population. The white-cell count, differential count, and blood levels of electrolytes and lactate dehydrogenase were normal, as were test results for liver and kidney function; laboratory test results are shown in Table 1. A screening test for human immunodeficiency virus types 1 and 2 was negative.

Dr. Huang: Two months later, whole-body ^{18}F-fluorodeoxyglucose (FDG) positron-emission tomography (PET)–CT performed at the first hospital reportedly showed that the skeleton had a diffusely heterogeneous appearance, with FDG uptake in both humeri, the left radius, and both acetabula (Fig. 1C and 1D). Gadolinium-enhanced MRI performed 1 month later showed multiple enhancing marrow-replacing lesions in the left humerus (Fig. 1E and 1F), the left ilium, and both acetabula (Fig. 2A and 2B). These findings were suggestive of multiple myeloma, metastases, or an infiltrative process. The lesions in the right kidney had not changed since the previous MRI.

Dr. Stone: Three months later, the patient was evaluated at the rheumatology clinic of this hospital. On review of systems, she reported fatigue, as well as pain in the left shoulder and arm that had lasted for several months. She reported no weight change, fever, chills, or cardiac, respiratory, gastrointestinal, or genitourinary symptoms. Her medical history was notable for early menopause, which had occurred at 40 years of age and had been attributed to primary ovarian failure, as well as celiac disease, hyperlipidemia, hypertension, hiatal hernia, kidney stones, and migraines. Medications included atorvastatin, spironolactone, topiramate, and a multivitamin. She reported having adverse reactions to meperidine, methylprednisolone, and nickel.

The patient was self-employed and lived in a small town with her husband. She had one adult child. She had smoked one third of a pack of cigarettes per day for 10 years but had quit smoking more than 15 years before this evaluation. She had no history of alcohol or other substance use. Her mother had died in her 50s from renal-cell carcinoma. A maternal aunt had ovarian and uterine cancer, and another had ovarian cancer. The patient's *BRCA* mutation status was negative.

On examination, the temporal temperature was 36.7°C, the heart rate 63 beats per minute, the blood pressure 134/61 mm Hg, and the oxygen saturation 97% while the patient was breathing ambient air. The weight was 90 kg, and the body-mass index (the weight in kilograms divided by the square of the height in meters) was 30.1. She had no proptosis, enlargement of the lacrimal glands, or enlargement of the major salivary glands (submandibular or parotid). No lymphadenopathy was present. The cardiac, lung, and abdominal examinations were unremarkable.

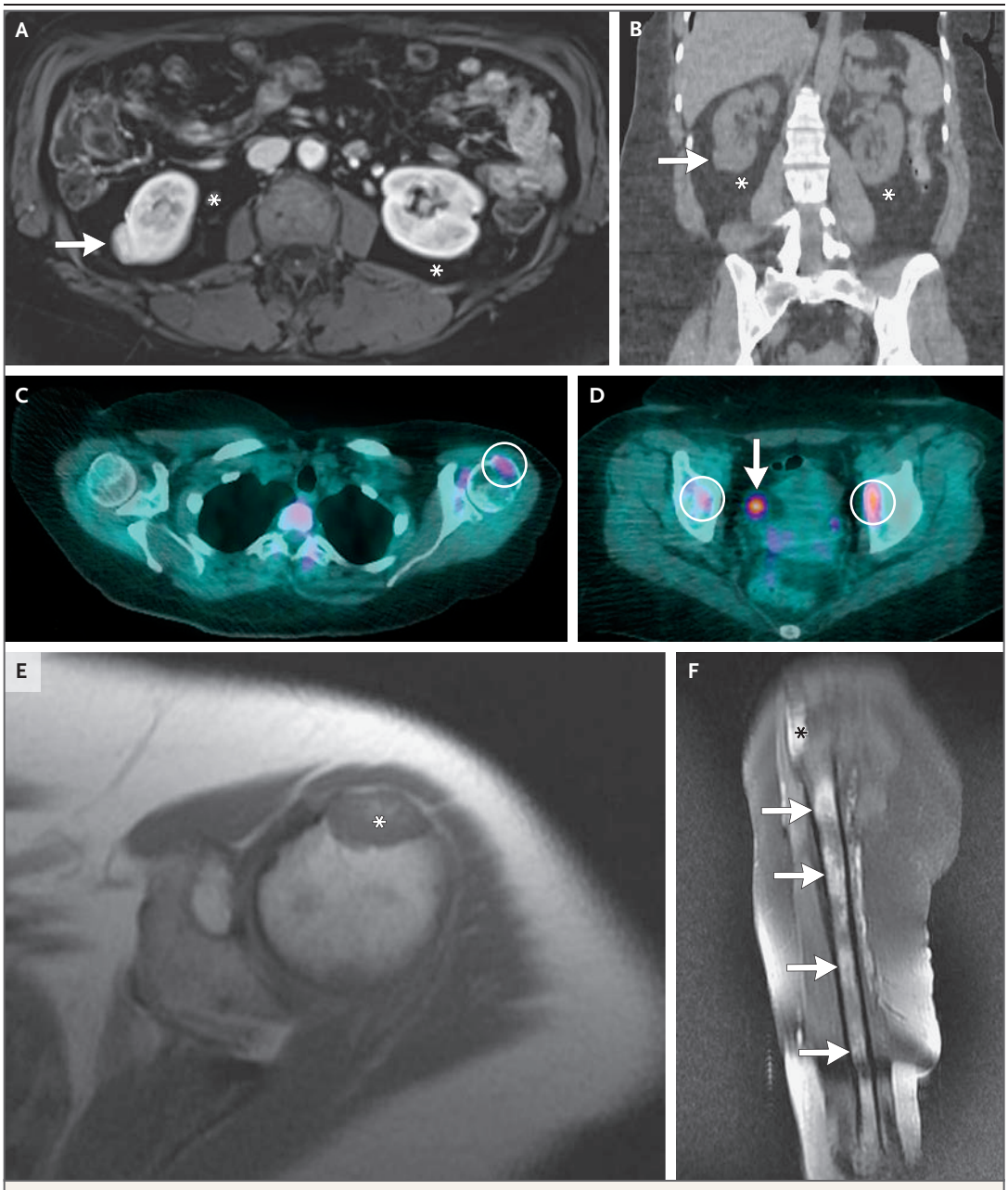

Figure 1. Initial imaging Studies.

An axial T1-weighted image obtained on gadolinium-enhanced MRI (Panel A) and a coronal reformatted image obtained during CT-guided biopsy (Panel B) show an exophytic, enhancing lesion arising from the lower pole of the right kidney (arrows). The perirenal and retroperitoneal fat appears normal (asterisks). Axial fused PET-CT images obtained through the upper chest and pelvis (Panels C and D, respectively) show lesions with ^{18}F-fluorodeoxyglucose (FDG) uptake in the left humeral head and both acetabula (circled). An additional focus of FDG uptake in the soft tissues of the right hemipelvis (arrow) indicates volume averaging of normal FDG activity within the urinary bladder. An axial T1-weighted image and a sagittal T1-weighted fat-suppressed image obtained on gadolinium-enhanced MRI (Panels E and F, respectively) show an enhancing lesion with low T1 signal intensity in the left humeral head (asterisks), a finding that corresponds to an FDG-avid lesion seen on PET-CT. Numerous additional enhancing lesions are present throughout the humeral shaft (arrows).

Table 1. Laboratory Data.

Variable	Reference Range, Adults, Third Hospital	7 Mo before Current Presentation, Third Hospital	Reference Range, Adults, This Hospital*	On Current Presentation, This Hospital	5 Mo after Current Presentation, This Hospital
Hemoglobin (g/dl)	11.1–15.9	14.6	12.0–16.0	15.6	14.3
Hematocrit (%)	34.0–46.6	42.9	36.0–46.0	47.9	41.9
White-cell count (per μl)	3400–10,800	8600	4500–11,000	8700	9950
Platelet count (per μl)	150,000–450,000	275,000	150,000–400,000	253,000	231,000
Globulin (g/dl)	2.2–3.9	3.7	1.9–4.1	4.2	3.3
C-reactive protein (mg/liter)	0–10	6	0–8	4.8	4.3
Erythrocyte sedimentation rate (mm/hr)	0–32	23	0–20	29	30
Serum protein electrophoresis	No monoclonal protein band	No monoclonal protein band	No monoclonal protein band	Mild diffuse increase in gamma globulin	Mild diffuse increase in gamma globulin
Immunoglobulin (mg/dl)					
IgG	586–1602	1693	614–1295	1969	1593
IgG1	248–810	1137	382.4–928.6	1148.0	987.9
IgG2	130–555	256	241.8–700.3	303.1	216.3
IgG3	15–102	36	21.8–176.1	32.7	32.4
IgG4	2–96	267	3.9–86.4	296.5	275.4
IgA	87–352	103	69–309	107	95
IgM	26–217	153	53–334	158	148
IgE	6–495	45	—	—	—
Free kappa light chain (mg/dl)	3.3–19.4	73.7	3.3–19.4	72.2	64.3
Free lambda light chain (mg/dl)	5.7–26.3	41.3	5.7–26.3	39.7	40.7
Kappa:lambda ratio	0.26–1.65	1.78	0.26–1.65	1.82	1.58
C3 (mg/dl)	82–167	135	81–157	130	229
C4 (mg/dl)	12–38	23	12–39	27	23
$Beta_2$-microglobulin (mg/liter)	0.6–2.4	2.9	—	—	—
Antinuclear antibody	Negative	Negative	Negative	—	—

* Reference values are affected by many variables, including the patient population and the laboratory methods used. The ranges used at Massachusetts General Hospital are for adults who are not pregnant and do not have medical conditions that could affect the results. They may therefore not be appropriate for all patients.

The musculoskeletal examination revealed tenderness and markedly limited abduction at the left shoulder but was otherwise unremarkable. The white-cell count, differential count, and blood levels of electrolytes, calcium, and albumin were normal, as were test results for liver and kidney function; laboratory test results are shown in Table 1.

Dr. Huang: A radiograph of the left shoulder showed a lytic lesion in the greater tuberosity that corresponded to lesions that had been identified on PET-CT and MRI (Fig. 2C). Three months later, repeat whole-body PET-CT performed at the first hospital reportedly showed FDG uptake in both humeri and both acetabula. No hypermetabolic lymph nodes or lytic bone lesions were reportedly present on CT.

Dr. Stone: A CT-guided bone biopsy of the left humerus performed at the first hospital reportedly showed fragments of trabecular bone. The bone marrow contained a lymphohistiocytic infiltrate with many plasma cells and fibrosis.

Immunostaining showed a high background level of kappa and lambda immunoglobulin light chains, without a clonal population, as well as scattered IgG4+ cells.

Five months after the initial presentation, the patient returned to the rheumatology clinic of this hospital. Laboratory test results are shown in Table 1. Testing for hepatitis B surface antigen and hepatitis C antibody was negative, as was an interferon-γ release assay for *Mycobacterium tuberculosis*. Two doses of rituximab were prescribed, but the patient had an infusion reaction while the second dose was being administered and was unable to complete the course.

Dr. Huang: Four months later, whole-body MRI performed at the first hospital reportedly showed multiple 2-to-3-cm lesions in the humeri and acetabula that had not changed substantially from previous imaging studies. Additional 3-cm lesions were noted in the distal femurs, proximal tibias, and proximal fibulas (Fig. 2D and 2E); these findings had not been seen previously.

Dr. Stone: Histopathological examination of a biopsy specimen and aspirate of a left tibial lesion was performed at the first hospital. Polytypic light-chain expression was noted, with more than 30 IgG4+ plasma cells per high-power field and an IgG4:IgG ratio of greater than 40%.

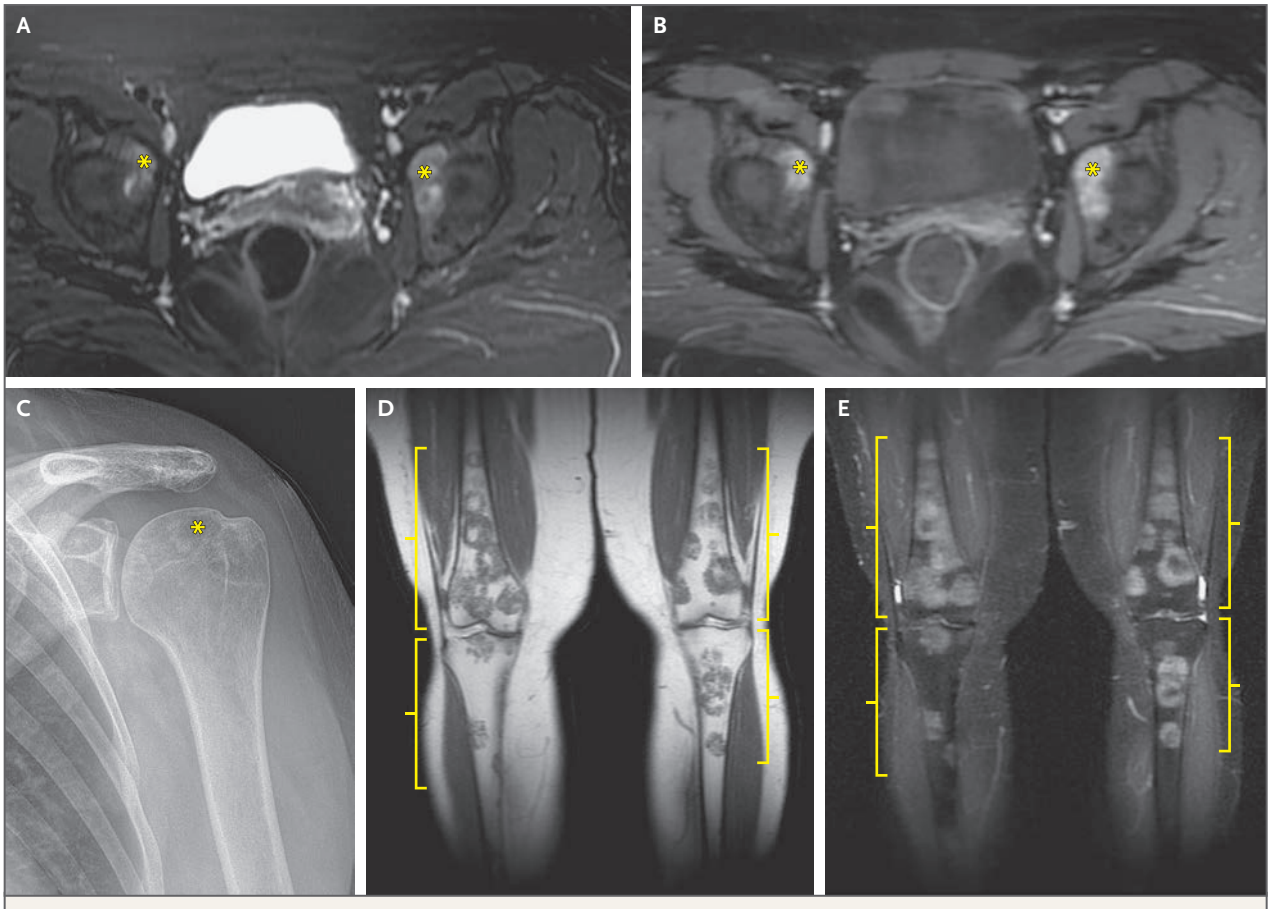

Figure 2. Additional Imaging Studies.

An axial T2-weighted fat-suppressed image and an axial T1-weighted image obtained on gadolinium-enhanced MRI (Panels A and B, respectively) show enhancing lesions with high T2 signal intensity in the acetabula (asterisks), findings that correspond to FDG-avid lesions seen on PET-CT. A radiograph of the left shoulder (Panel C) shows a lytic lesion in the humeral head (asterisk) that corresponds to a lesion identified on MRI and PET-CT. A coronal T1-weighted image and a coronal T2-weighted fat-suppressed image obtained on MRI (Panels D and E, respectively) show numerous lesions of the distal femurs and proximal tibias (brackets) with low T1 signal intensity and high T2 signal intensity.

Table 2. Causes of Polyclonal Hypergammaglobulinemia.

Category	Examples	Likelihood in This Patient
Liver disease	Autoimmune hepatitis, fatty liver, or viral hepatitis	Ruled out: normal test results for liver function, normal albumin levels, and unremarkable liver imaging
Iatrogenic cause	Use of immunoglobulin replacement therapy, in the absence of baseline polyclonal hypergammaglobulinemia, for indications such as neurologic conditions or immune thrombocytopenia	Ruled out: no use of intravenous or subcutaneous immunoglobulin therapy
Immunodeficiency	Autoimmune lymphoproliferative syndrome or activated phosphoinositide 3 kinase delta syndrome	Very unlikely: no history of fever or infection, no lymphadenopathy or hepatosplenomegaly, and the age at presentation
Infection	Human immunodeficiency virus infection, Epstein–Barr virus infection, *Mycobacterium tuberculosis* infection, or leishmaniasis	Unlikely: no fever, normal C-reactive protein level, negative cultures, no evidence of granulomas or organisms on four biopsies, long disease course, and no lymphadenopathy or hepatosplenomegaly
Nonhematologic cancer	Cancer associated with inflammation and accompanied by a high C-reactive protein level	Very unlikely: no evidence of cancer on four biopsies, long disease course, no pain, and no cortical bone destruction on imaging
Autoimmune or autoinflammatory disease	Sarcoidosis, eosinophilic granulomatosis with polyangiitis, Sjögren's syndrome, SAPHO syndrome (synovitis, acne, pustulosis, hyperostosis, and osteitis), or chronic recurrent multifocal osteomyelitis	Unlikely: no fever, normal C-reactive protein level, and negative tests for autoantibodies
IgG4-related disease	Disease commonly manifesting as swelling of the lacrimal and salivary glands, autoimmune pancreatitis, and retroperitoneal fibrosis; the elevated IgG4 level can cause beta–gamma bridging on serum protein electrophoresis	Possible, but with a very atypical presentation: extensive bone involvement without involvement of other, common organs (glands, pancreas, and lymph nodes) and a lack of response to rituximab
Hematologic disorder	Castleman's disease, lymphoma (angioimmunoblastic T-cell lymphoma or Hodgkin's lymphoma), or histiocytic disorder (Rosai–Dorfman–Destombes disease or Erdheim–Chester disease)	Unlikely: Castleman's disease (given the normal C-reactive protein level, presence of bone lesions, and absence of lymphadenopathy) and lymphoma (no lymphadenopathy or cortical bone destruction on imaging) Likely: histiocytic disorder

Diagnostic tests were performed, and management decisions were made.

DIFFERENTIAL DIAGNOSIS

Dr. Luke Y.C. Chen: This 45-year-old woman presented to the rheumatology clinic of this hospital with a 2-year history of bilateral kidney and bone lesions. She reported fatigue and pain in the left shoulder but no fever, chills, or weight loss. An excisional tissue specimen from the left kidney and core-biopsy specimens from the retroperitoneum, left humerus, and left tibia obtained over the course of her illness showed lymphoplasmacytic infiltrates, fibrosis, and variably increased levels of IgG4+ plasma cells. Notable laboratory findings included repeat normal C-reactive protein levels and persistent mild polyclonal hypergammaglobulinemia with a mildly elevated IgG4 level.

The patient had been referred to the rheumatology clinic for what was thought to be IgG4-related disease, specifically IgG4-related retroperitoneal fibrosis, and was treated with rituximab. However, many aspects of this case are atypical for IgG4-related disease, and several diseases can mimic or be mimicked by IgG4-related disease, including vasculitis, granulomatous disease, cancer, and various hematologic conditions.[1]

A feature of this case that can be used to formulate a broad yet appropriately focused differential diagnosis is polyclonal hypergammaglobulinemia. Polyclonal hypergammaglobulinemia with an elevated IgG level can be divided into eight major categories (Table 2).[2] The history, findings on physical examination, and results of routine laboratory tests — such as measurement of liver enzyme levels, autoantibody tests, and viral serologic tests — can help in identifying the appropriate category.

The differential diagnosis can be further refined by considering the C-reactive protein level. Polyclonal hypergammaglobulinemia is largely driven by interleukin-6 in inflammatory processes,[3] which are characterized by a high C-reactive protein level. When the C-reactive protein level is normal, polyclonal hypergammaglobulinemia may instead be driven by another process. For example, loss of hepatic filtration leads to increased exposure to enteric antigens and endotoxins, which can result in polyclonal hypergammaglobulinemia; polyclonal hypergammaglobulinemia can also result from complex immune dysregulation in the context of IgG4-related disease or inborn errors of immunity.

IgG subclass levels can be a helpful clue. IgG subclasses are named in order of natural abundance, and an elevated IgG1 level is commonly seen in patients with autoimmune disease, infection, or liver disease.[2,4] A markedly elevated serum IgG4 level (>500 mg per deciliter) is approximately 90% specific for IgG4-related disease, but mildly elevated levels (such as the level seen in this patient, 297 mg per deciliter) can be seen in many different disease states.

UNLIKELY OR RULED-OUT CAUSES

Liver disease and iatrogenic causes can be ruled out in this case because no evidence of these conditions was found in the history or on physical examination, laboratory testing, or imaging studies. Hereditary or acquired immunodeficiencies are very unlikely because the patient was 45 years of age at presentation and did not have a fever, a high C-reactive protein level, or evidence of infection. Furthermore, the protracted presentation (over 2 years), the absence of a histologic diagnosis despite four biopsies, the absence of bone pain despite numerous bone lesions, and the absence of cortical bone destruction on imaging make nonhematologic cancer very unlikely.

AUTOIMMUNE OR AUTOINFLAMMATORY DISEASE

An autoimmune disease that commonly causes polyclonal hypergammaglobulinemia is Sjögren's syndrome. However, the patient did not have sicca symptoms, arthritis or synovitis, autoantibodies, or other features of typical autoimmune disease, which makes the diagnosis unlikely. Autoinflammatory diseases that affect bone, such as SAPHO syndrome (characterized by synovitis, acne, pustulosis, hyperostosis, and osteitis) and chronic recurrent multifocal osteomyelitis, should be considered. However, patients with SAPHO syndrome nearly always have involvement of the sternum and clavicles, which was not seen in this patient, and other autoinflammatory conditions involving bone are usually mediated by interleukin-1, type I interferonopathies, or nuclear factor κB (tumor necrosis factor) and are therefore characterized by fever and an elevated C-reactive protein level.[5,6]

IGG4-RELATED DISEASE

IgG4-related disease was first described in 2001 and is an important cause of retroperitoneal fibrosis.[7] The serum IgG4 level is elevated in approximately 65 to 70% of affected patients. Although the polyclonal hypergammaglobulinemia with a normal C-reactive protein level, the mildly elevated serum IgG4 level (297 mg per deciliter), the retroperitoneal fibrosis, and the increased level of IgG4+ plasma cells in tissue seen in this patient are features suspicious for IgG4-related disease, several features of this case are not consistent with this diagnosis. First, bone involvement is exceedingly rare in IgG4-related disease, except for involvement of the maxillofacial bones (eosinophilic angiocentric fibrosis), and extensive involvement of the appendicular skeleton has not been reported. Second, most patients with advanced IgG4-related disease have involvement of other organs, such as the lymph nodes, pancreas, and lacrimal, salivary, and parotid glands. Third, more than 95% of patients with IgG4-related disease have a clinically significant response to rituximab, yet new lesions developed in this patient shortly after she had received 1 g of rituximab.[8]

Furthermore, the findings on biopsy in this patient do not support a diagnosis of IgG4-related disease. The 2012 International Consensus Criteria (ICC) outline the thresholds for the diagnosis of IgG4-related disease in typical target organs,

which range from 10 IgG4+ plasma cells per high-power field in the meninges to 100 IgG4+ plasma cells per high-power field in the salivary glands. Regardless of the organ, the ratio of IgG4+ to IgG+ plasma cells is more than 40%. Examination of this patient's retroperitoneal tissue showed more than 10 IgG4+ plasma cells per high-power field with an IgG4:IgG ratio of less than 40%, results that fall short of the thresholds established for needle biopsy of retroperitoneal tissue (30 IgG4+ plasma cells per high-power field and an IgG4:IgG ratio of >40%).[9] The tibial biopsy specimen had greater enrichment — more than 30 IgG4+ plasma cells per high-power field with an IgG4:IgG ratio of more than 40% — but the 2012 ICC thresholds do not include thresholds for bone, and in fact, the 2019 American College of Rheumatology–European League Against Rheumatism diagnostic criteria list long-bone involvement as an exclusion criterion for IgG4-related disease.[10] Thus, IgG4-related disease is an unlikely diagnosis in this patient.

HEMATOLOGIC DISORDERS

Three hematologic conditions should be included in the differential diagnosis: lymphoma, Castleman's disease, and histiocytic disorders. Primary lymphoma of bone caused by diffuse large B-cell lymphoma is usually an aggressive cancer associated with pain and evidence of bone destruction on imaging, and it is not likely to be missed on four separate biopsies. Non-Hodgkin's lymphoma with bone metastasis would also have a more aggressive course than that seen in this case and would be associated with pain, lymphadenopathy, and evidence of bone destruction on imaging. Hodgkin's lymphoma can have renal and retroperitoneal involvement and may elude histologic diagnosis, given that the pathognomonic Reed–Sternberg cells may be rare within affected tissue. However, Hodgkin's lymphoma nearly always manifests with lymphadenopathy, and bone and renal involvement is rare.

Castleman's disease is an important consideration in a patient with polyclonal hypergammaglobulinemia. Although unicentric Castleman's disease often manifests as a retroperitoneal mass and can be associated with a normal C-reactive protein level, it would not cause numerous bone lesions. In multicentric Castleman's disease, lymphadenopathy and a high C-reactive protein level are nearly obligatory features, and extensive bone disease is very unlikely. Therefore, Castleman's disease can essentially be ruled out in this case.

The prominence of the bone lesions in this patient makes a histiocytic disorder highly likely.[11] Both Erdheim–Chester disease (ECD) and Rosai–Dorfman–Destombes disease (RDD) may manifest with polyclonal hypergammaglobulinemia.[12] Bone lesions are present in more than 95% of cases of ECD, occurring more often in the long bones of the appendicular skeleton than in the axial skeleton. Bone lesions in ECD are typically symmetric and sclerotic, have increased tracer uptake on technetium-99m scintigraphy or PET-CT, and are typically associated with pain at affected sites. The histologic diagnosis of ECD is notoriously difficult. Findings may vary from anatomical site to site, and the classic infiltrate of foamy histiocytes — which is positive for CD68, CD163, and FXIII, with Touton giant cells; negative for CD1a; and negative or weakly positive for S100 — may be missed on needle biopsy. In many cases, only nonspecific inflammatory or fibrotic changes are seen. ECD can cause retroperitoneal fibrosis, typically in the form of perinephric fat infiltration with a "hairy kidney" appearance on CT or MRI. This patient's extensive appendicular skeletal involvement and retroperitoneal fibrosis place ECD high on the differential diagnosis. However, her bone lesions are lytic rather than sclerotic, and although she has many bone lesions, she has reported pain only in the left shoulder. Polyclonal hypergammaglobulinemia and increased levels of IgG4+ plasma cells in tissue have been reported in patients with ECD, but these findings are relatively rare.

Thus, RDD should be considered. RDD is an R group histiocytosis that typically affects lymph nodes and soft tissue. Histiocytoses are divided into five groups, with the R group including the RDD spectrum of disorders, which are characterized by frequent immune dysregulation, as well as mutations in the mitogen-activated protein kinase (MAPK) pathway in approximately 40% of cases. On histologic examination, RDD is characterized by large histiocytes with pale cytoplasm and frequent emperipolesis of plasma cells and lymphocytes. Emperipolesis is a biologic process in which an intact cell is found within the cytoplasm of another cell and, unlike

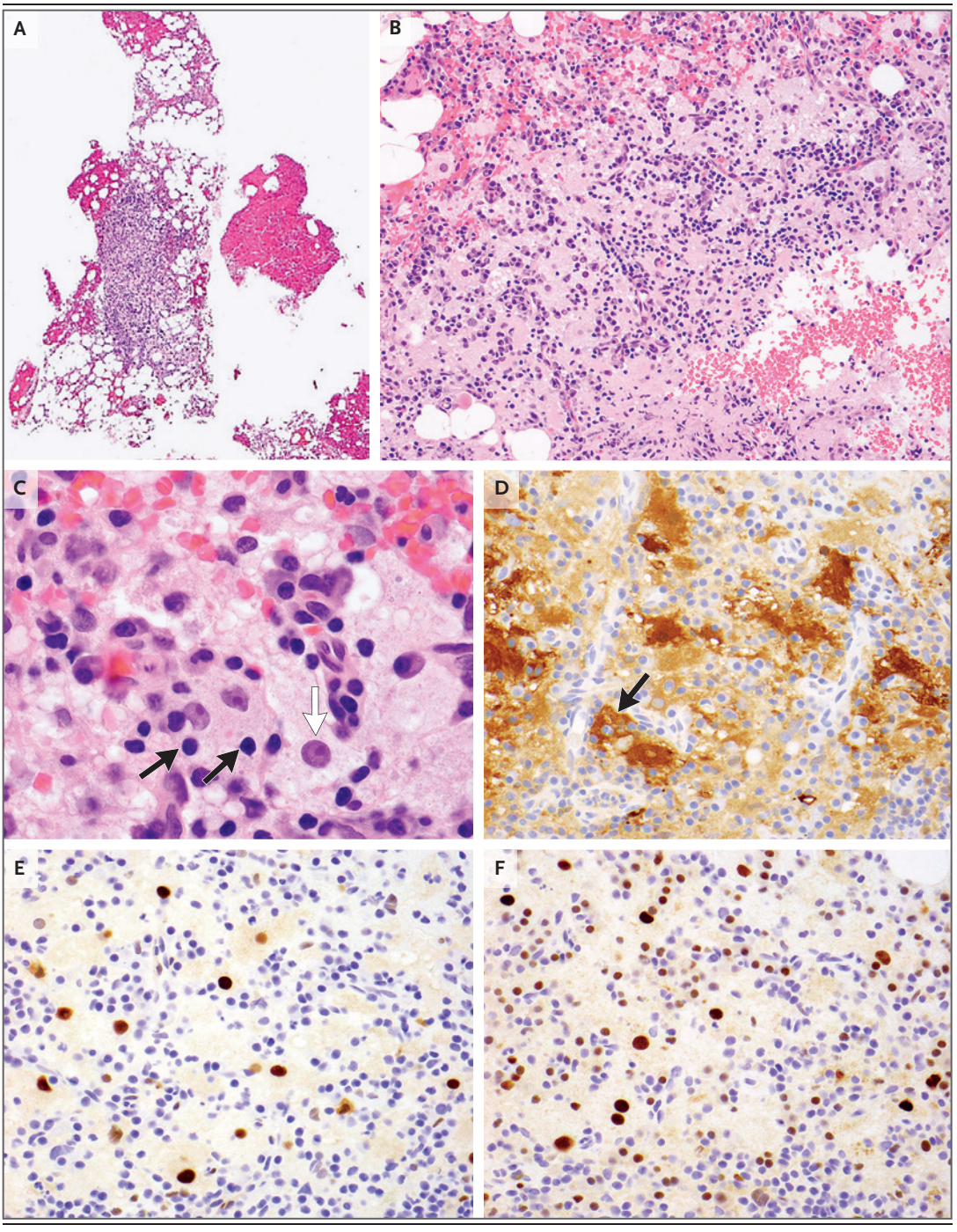

in phagocytosis, is not destroyed. The histiocytes are positive for CD68 and S100 and negative for CD1a. In past reports, bone involvement was observed in less than 10% of cases of RDD. However, bone involvement in RDD has been underestimated because it is often subclinical, and CT lacks the sensitivity to detect it. PET-CT and MRI are more sensitive than CT alone. The bone lesions are FDG avid, and MRI often reveals lytic or mixed lytic and sclerotic bone lesions. A recent study performed with the use of PET-CT showed bone involvement in 18 of 64 patients (28%).[13]

Figure 3 (facing page). Tibial-Biopsy Specimen.
A biopsy specimen of the left medial tibia includes small fragments of marrow with hypocellular, fatty areas and focal hypercellular areas (Panel A). At higher magnification, a hypercellular area shows a mixture of many histiocytes, small lymphocytes, and plasma cells (Panel B). Multiple histiocytes have round-to-oval nuclei, distinct nucleoli, and abundant pale cytoplasm (Panel C, white arrow). Some histiocytes appear to contain intact small lymphocytes within their cytoplasm, a feature known as emperipolesis (Panel C, black arrows). The distinctive histiocytes are positive for S100, and their cytoplasm has occasional small lymphocytes that are negative for S100 (Panel D, black arrow); these findings are consistent with emperipolesis. Staining for cyclin D1 is positive in the nuclei of the histiocytes (Panel E), a finding that suggests activation of the mitogen-activated protein kinase (MAPK) pathway. Staining for OCT2 is positive in the nuclei of the histiocytes, as well as in the nuclei of admixed small B cells and plasma cells (Panel F).

Pain has been reported in patients with spine and pelvic disease, but not in those with appendicular skeletal involvement.[13]

Whereas 50 to 60% of patients with ECD are positive for the *BRAF* V600E mutation, most patients with RDD have no mutations. A subset of patients with RDD have driver mutations in genes of the MAPK pathway, including *KRAS* and *MAP2K1*, which are amenable to targeted therapy with MEK inhibitors.[11] The diagnostic test I would recommend in this case is a careful review of all four biopsy specimens, with particular attention to features of histiocytosis. Immunohistochemical staining for CD1a, CD68, CD163, S100, and BRAF may be helpful, along with molecular studies for the *BRAF* V600E mutation and next-generation sequencing.

DR. LUKE Y.C. CHEN'S DIAGNOSIS

Rosai–Dorfman–Destombes disease of the bone, kidneys, and retroperitoneum.

PATHOLOGICAL DISCUSSION

Dr. Judith A. Ferry: The first specimen reviewed at this hospital, approximately 1 month before the patient's presentation to the rheumatology clinic, was submitted as a biopsy specimen of the right kidney. Microscopic examination revealed soft tissue with fibrosis and a cellular infiltrate with abundant plasma cells, histiocytes, and small lymphocytes, but there was no renal parenchyma. The specimen was thus thought to be retroperitoneal soft tissue. The fibrosis had a storiform pattern focally. Immunostaining showed more than 10 IgG4+ plasma cells per high-power field with an IgG4:IgG ratio of less than 40%. Overall, although the IgG4:IgG ratio was below the usual threshold, the findings were considered to be consistent with IgG4-related disease.

Given the subsequent clinical course, the retroperitoneal biopsy specimen was reviewed again, and additional routinely stained slides and immunostains were prepared. The specimen showed rare histiocytes with large oval nuclei, distinct nucleoli, and abundant pale cytoplasm. The histiocytes were positive for S100, and some had an appearance that was suggestive of emperipolesis. Plasma cells were polytypic, with a mixture of kappa-positive and lambda-positive plasma cells.

A biopsy specimen of the left humerus was reviewed and showed bone with a lymphohistiocytic infiltrate with many plasma cells and fibrosis. The histologic and immunophenotypic findings overlapped with those of the retroperitoneal biopsy specimen, but the findings were not considered to be diagnostic of a specific disease. It is notable that the patient was reported to have lytic bone lesions, but trabecular bone was seen throughout the biopsy specimen; this discrepancy suggests that the biopsy results might not have been optimally representative of the patient's disease process.

A biopsy specimen of the left medial tibia was reviewed and showed scant bone and fragments of marrow, with some areas replaced by a dense infiltrate of small lymphocytes, plasma cells, and clustered histiocytes in a fibrillar background (Fig. 3A and 3B). The histiocytes were large, with enlarged round-to-oval nuclei, distinct amphophilic nucleoli, and abundant pale, finely granular cytoplasm, and some had an appearance that was suggestive of emperipolesis (Fig. 3C). Flow cytometry showed no diagnostic abnormalities. Cytogenetic analysis was limited by a low mitotic index, but no cytogenetic abnormalities were identified. Immunostaining showed many CD138+ plasma cells, which were mostly positive for IgG. Less than 40% of the IgG+ cells were IgG4+ plasma cells. The plasma cells were polytypic. The large histiocytes were positive for

S100; this immunostain confirmed the presence of emperipolesis (Fig. 3D). The large histiocytes also showed strong nuclear staining for OCT2 and cyclin D1 (Fig. 3E and 3F). This immunoprofile is characteristic of RDD.[14] The findings in the tibia were interpreted as features of RDD. Because of the overlap in histologic features, the retroperitoneal specimen and the humeral specimen were considered to be involved by the same process. Osseous involvement in RDD is rare but has been described.[15]

PATHOLOGICAL DIAGNOSIS

Rosai–Dorfman–Destombes disease of the bone and retroperitoneum.

DISCUSSION OF MANAGEMENT AND FOLLOW-UP

Dr. Stone: There are various treatment options for systemic RDD, and treatment must be tailored to the individual patient's situation.[16,17] A strategy involving observation alone may be suitable for asymptomatic disease of the lymph nodes or skin, because some patients with such disease have spontaneous remission. Surgical resection is suitable for unifocal disease, which is rare, and debulking may be necessary for large masses that threaten the airway or impinge on critical organs. Most patients, however, receive systemic therapy. Glucocorticoid therapy can be useful for nodal disease, but single-agent treatment is generally not adequate for disease that involves extranodal tissues. The discovery of driver mutations in the MAPK pathway in patients with RDD has dramatically altered the treatment landscape. In this case, next-generation sequencing was performed, and the patient was found to have a mutation in *MAP2K1*. The overall response to treatment with a MEK inhibitor, such as cobimetinib or trametinib, is nearly 90% among patients with a known mutation, and many patients with wild-type disease also have a response.[18]

This patient was treated with a daily dose of cobimetinib, and after 6 months of therapy, she had a complete clinical response with resolution of symptoms. Follow-up PET-CT showed a complete radiologic response, as well. The patient completed her treatment course approximately 1 year ago, and she continues to do well.

FINAL DIAGNOSIS

Rosai–Dorfman–Destombes disease.

This case was presented at the Harvard Medical School course "Advances in Rheumatology 2023," directed by Drs. John H. Stone and Michael E. Weinblatt.

Disclosure forms provided by the authors are available with the full text of this article at NEJM.org.

REFERENCES

1. Chen LYC, Mattman A, Seidman MA, Carruthers MN. IgG4-related disease: what a hematologist needs to know. Haematologica 2019;104:444-55.
2. Zhao EJ, Cheng CV, Mattman A, Chen LYC. Polyclonal hypergammaglobulinaemia: assessment, clinical interpretation, and management. Lancet Haematol 2021;8(5):e365-e375.
3. Brandt SJ, Bodine DM, Dunbar CE, Nienhuis AW. Dysregulated interleukin 6 expression produces a syndrome resembling Castleman's disease in mice. J Clin Invest 1990;86:592-9.
4. Zhao EJ, Carruthers MN, Li CH, Mattman A, Chen LYC. Conditions associated with polyclonal hypergammaglobulinemia in the IgG4-related disease era: a retrospective study from a hematology tertiary care center. Haematologica 2020;105(3):e121-e123.
5. Chen L, Fajgenbaum DC. Castleman disease. In: Stone JH, ed. A clinician's pearls and myths in rheumatology. Cham, Switzerland: Springer International Publishing, 2023 (https://link.springer.com/10.1007/978-3-031-23488-0_51).
6. Nigrovic PA, Lee PY, Hoffman HM. Monogenic autoinflammatory disorders: conceptual overview, phenotype, and clinical approach. J Allergy Clin Immunol 2020;146:925-37.
7. Katz G, Stone JH. Clinical perspectives on IgG4-related disease and its classification. Annu Rev Med 2022;73:545-62.
8. Carruthers MN, Topazian MD, Khosroshahi A, et al. Rituximab for IgG4-related disease: a prospective, open-label trial. Ann Rheum Dis 2015;74:1171-7.
9. Deshpande V, Zen Y, Chan JK, et al. Consensus statement on the pathology of IgG4-related disease. Mod Pathol 2012;25:1181-92.
10. Wallace ZS, Naden RP, Chari S, et al. The 2019 American College of Rheumatology/European League Against Rheumatism classification criteria for IgG4-related disease. Ann Rheum Dis 2020;79:77-87.
11. McClain KL, Bigenwald C, Collin M, et al. Histiocytic disorders. Nat Rev Dis Primers 2021;7:73.
12. Estrada-Veras JI, O'Brien KJ, Boyd LC, et al. The clinical spectrum of Erdheim-Chester disease: an observational cohort study. Blood Adv 2017;1:357-66.
13. Goyal G, Ravindran A, Young JR, et al. Clinicopathological features, treatment approaches, and outcomes in Rosai-Dorfman disease. Haematologica 2020;105:348-57.
14. Ravindran A, Goyal G, Go RS, Rech KL. Rosai-Dorfman disease displays a unique monocyte-macrophage phenotype characterized by expression of OCT2. Am J Surg Pathol 2021;45:35-44.

15. Demicco EG, Rosenberg AE, Björnsson J, Rybak LD, Unni KK, Nielsen GP. Primary Rosai-Dorfman disease of bone: a clinicopathologic study of 15 cases. Am J Surg Pathol 2010;34:1324-33.
16. Abla O, Jacobsen E, Picarsic J, et al. Consensus recommendations for the diagnosis and clinical management of Rosai-Dorfman-Destombes disease. Blood 2018;131:2877-90.
17. Go RS, Jacobsen E, Baiocchi R, et al. Histiocytic neoplasms, version 2.2021, NCCN clinical practice guidelines in oncology. J Natl Compr Canc Netw 2021;19:1277-303.
18. Diamond EL, Durham BH, Ulaner GA, et al. Efficacy of MEK inhibition in patients with histiocytic neoplasms. Nature 2019;567:521-4.